

## Two-step degenerate four-wave mixing as a means to decrease pre- and post-filtering effects in optically thick media

P. Ljungberg, O. Axner

The Analytical Laser Spectroscopy Group, Department of Physics, Chalmers University of Technology and The University of Göteborg, S-412 96 Göteborg, Sweden  
(Fax: +46-31/7723496)

Received 19 October 1993/Accepted 7 March 1994

**Abstract.** The use of crossed beam 2-Step Degenerate Four-Wave Mixing (2S-DFWM) for decreasing pre- and post-filtering effects under optically thick conditions has been investigated. 2S-DFWM is a technique in which the DFWM process is performed between two excited states of which the lower one is populated by an ordinary laser excitation from a low lying, highly populated state. Experiments were performed on Au in an acetylene/air flame. We have shown that under conditions where ordinary (one-step) DFWM experiments are significantly affected by pre- and post-filtering effects (i.e., partly absorption of the pump, probe or signal beams prior to or after the interaction region) the 2S-DFWM technique can give virtually interference free signals. A variety of different laser beam and flame configurations have been investigated. It was found that the use of a crossed beam geometry, where the first step exciting laser is incident upon the interaction region perpendicular to the DFWM beams, completely eliminated severe pre- and post-filtering effects occurring for an ordinary single-step DFWM scheme in an optically thick medium.

**PACS:** 35.80, 42.65.Ky, 82.80

Degenerate Four-Wave Mixing (DFWM) is a non-linear laser-based spectroscopic technique that produces a coherent, spectrally narrow-banded, and highly collimated signal beam by the mixing of three input beams (all resonant with a transition) in a species under study. The technique has recently shown powerful capabilities for detection of a variety of species within a wide range of applications [1, 2]. The main reasons for the increasing interest in the DFWM technique lately are its extraordinary properties, some of which are non-intrusiveness, species selectivity, high sensitivity, highly directional output signal and a rather low vulnerability to collisions. These properties, which can be seen as a fortuitous combination of some of the most powerful advantages of Laser-Induced Fluorescence (LIF) (e.g., high sensitivity) [3–6] with others of Coherent Anti-Stokes Raman Scat-

tering (CARS) (e.g., a highly directional output signal) [7, 8], make the technique potentially useful for studies of species concentrations and local combustion temperatures for applications primarily within the field of combustion diagnostics [2] since they allow measurements of the signal in a location far from the interaction region (several meters), permit efficient rejection of potentially interfering radiation (e.g., emission, fluorescence, scattered laser light, etc.) as well as the use of small optical ports for input and output access. In addition, although nonlinear processes are generally considered to be rather weak, the DFWM technique has a high sensitivity for a number of species since it is performed on a (strong) resonant transition.

The DFWM technique has so far been used for detection of inherently produced combustion radicals/products in flames (e.g., OH [9–13], NO [14], CO [15] and NH [11]), molecules in cells or jets (e.g., I<sub>2</sub> [16–18], SF<sub>6</sub> [19], HCO [20], HF [21] and eosin [17]) as well as atoms (Na) seeded into flames [22–24] and cells [25, 26]. In addition, two-dimensional imaging studies (of Na [24], OH [27] and NO<sub>2</sub> [28]), multiplex (i.e., broad-band) detection (of OH [29] and Na [30]), as well as Doppler-free studies of various species have been performed [2, 31–33]. In addition, a theoretical description of the DFWM process has been pursued by several authors [1, 26, 34–40]. However, much of the characterization of the DFWM technique remains – a characterization which is needed for an assessment of the full practical applicability of the technique within the area of combustion diagnostics.

Partly due to the high sensitivity, the DFWM signal has been found to be affected by absorption processes in the medium to be studied. These absorption processes include absorption of the pump or the probe beams (below called pre-filtering effects), or the signal beam (below called post-filtering effects), by the species under consideration. Pre- and post-filtering effects can thus occur if the species to be studied has a sufficiently large absorption cross-section and exists in high enough concentrations. These types of effects appear normally as a

dip in the signal on resonance as the wavelength of the laser is scanned across the transition.

Such a dip can originate from pre- and post-filtering effects, from saturation of the transitions or from ac-Stark effects (for strong laser beams). The pre- and post-filtering effects can most conveniently be distinguished from the other ones by a study of the dependence of the signal shape upon laser light intensity. For low (or medium) intensities, the pre- and post-filtering effects dominate since these are only governed by the absorption cross-section of the transition used times the path lengths.

Pre- and post-filtering effects in media that are not optically thin have been known for long in other optical techniques (e.g., absorption, emission and fluorescence) and thus their behaviour is well documented in the literature [41–43]. These effects are, however, in general more pronounced in the DFWM technique than in other optical techniques due to the strong nonlinear behaviour of the DFWM process, and have been noticed by several workers previously [16, 24, 44]. However, no one has so far made any real attempt to reduce their influences.

In this paper, we have investigated the possibility to reduce pre- and post-filtering effects in media that are not completely optically thin (i.e., when species with high absorption cross-sections exist in sufficiently high concentrations) by performing DFWM between two excited states that both have low thermal populations. In order to obtain highest possible sensitivity of the technique, the lower level of the two is populated by a first step excitation from a low lying, highly populated state. This is below referred to as 2-Step DFWM (2S-DFWM).

A distinct advantage of the 2S-DFWM is thus an ability to reduce the influence of pre- and post-filtering effects. Other possible advantages are a decreased background and an increased signal strength, especially when the first resonant transition has a low transition probability or is excited by low light intensities (e.g., for transitions requiring far UV-light wavelengths that can be produced only at low intensities by modern laser systems or when large beam areas are used). There is also a possibility to obtain an improved spatial resolution through the use of crossed first and second step excitation beams.

DFWM from excited states has been carried out previously. For example, investigations of absorption and saturation effects on DFWM in excited states of Na formed during collisions, so called Excited-State DFWM (ESDFWM), were performed by Ewart et al. [45] as well as by Ewart and O’Leary [46–48] already in the early eighties. In the work by Ewart et al. [45], the laser was tuned to the resonance between two excited states whose frequency was in the extreme wing of the transition from the ground state to the lower of the two excited states. Hence, the same laser was used for both steps, implying that the authors had no possibility to separate, and thus investigate separately, the two processes of the first-step extreme-wing absorption and the second-step DFWM process. Ewart and O’Leary [46–48], on the other hand, excited sodium atoms to the 3p state on the extreme blue and red wings of the D-lines (in the presence of various

rare-gas atoms as perturbers) with light from one dye laser while a second dye laser provided the light for the DFWM between the 3p and 4d states in the atom.

Another more recent two-step DFWM experiment, which also has been termed Stimulated Emission Pumping Degenerate Four Wave Mixing (SEP-DFWM), has been done by Zhang et al. [49] on gaseous CS<sub>2</sub> under low-pressure conditions. In addition, Ljungberg and Axner [50] have investigated 2S-DFWM as a means to improve the signal strengths when species with low transition probabilities in the ordinary resonant excitation step are to be detected, or when only low light intensities can be produced at the wavelength of the ordinary resonant excitation transition.

The aim of the present work is thus to investigate whether 2S-DFWM is a feasible means to broaden the applicability of the DFWM technique by allowing for a background- and interference-free detection of species also under optically thick conditions.

## 1 Experimental setup and procedures

The experimental setup used in this work is presented in Fig. 1. A XeCl-excimer laser (Lambda Physik, LPX 210i) simultaneously pumped two dye lasers (Lambda Physik, FL 2003) with 250 mJ pulses of 308 nm light at a pulse frequency of 50 Hz. The dye lasers provided light in the visible wavelength regions using the dyes coumarin 153 (around 536 nm) and rhodamine 6G (around 585 nm). The light from the coumarin 153 dye laser was frequency doubled in a BBO crystal in order to produce UV light with wavelengths around 268 nm. Pulses from the dye lasers with energies up to approximately 150 μJ/pulse in the visible and 30 μJ/pulse in the UV region were used. The pulses had a duration of approximately 20 ns. For the single-step DFWM experiments the UV light produced in the BBO crystal was used directly for the DFWM process while for the 2S-DFWM experiments the UV light was used as a first exciting step while the rhodamine 6G dye in the second dye laser provided visible light for the DFWM process.

The DFWM laser beam was passed through an aperture in order to provide a circular beam profile with a

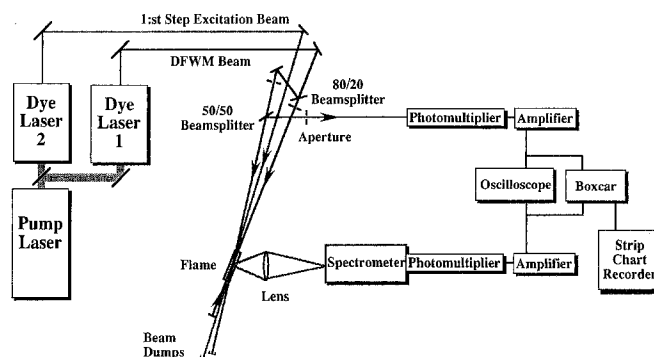


Fig. 1. Experimental setup for the ordinary (one-step) DFWM and 2S-DFWM experiments

diameter of 4 mm. Using a beam splitter, roughly 20% of the DFWM light was split off to provide a probe beam. This probe beam was passed through a second aperture to reduce its diameter to 2 mm and a 50/50 beamsplitter (which split off the counterpropagating signal beam) before traversing the flame. The remaining pump beam was retroreflected so as to give a counterpropagating backward pump beam. The probe and pump beams intersected each other in the center of the flame at an angle of  $3.5^\circ$ . Furthermore, when performing the 2S-DFWM experiments the first-step exciting laser beam was directed at the interaction region. This was done either in a direction bisecting the angle between the probe and pump beams, thus providing maximum overlap between the exciting and DFWM processes, or in a direction roughly perpendicular to the DFWM beams so as to maximize spatial resolution and minimize pre- and post-filtering effects. All laser beams could be attenuated through the use of neutral-density filters.

The flame was supported on a commercially available 10 cm single-slot burner head (Instrumentation Laboratory) that could be rotated in the horizontal plane. This allowed the DFWM beams to traverse the flame parallel or orthogonal to the burner head slot. The flame was fed with air and acetylene in roughly stoichiometric proportions. An aqueous solution of some tens or hundreds of ppm ( $\mu\text{g}/\text{mL}$ ) concentration of Au was aspirated into the flame. Only a certain fraction of the aspirated Au atoms were carried by the flame gases into the flame (approximately 5%), whereby the atomic concentration in the flame roughly corresponded to  $10^{11}$ – $10^{13}$  atoms per  $\text{cm}^3$ , depending on the actual degree of atomization for Au in the flame, nebulization efficiency, flame gas velocities, etc.

The signal beam, split off from the counterpropagating probe beam by the 50/50 beamsplitter, was directed

through an aperture placed in front of a 3 m long plastic tube at the end of which a photomultiplier (Hamamatsu R2027) registered the signal intensity. This arrangement minimized the influence of scattered light from the lasers and optics. Neutral density filters could be inserted in front of the aperture in order to attenuate the signal beam so as not to saturate the photomultiplier. The effect of these neutral density filters has been taken into consideration in all the data presented throughout this work.

Fluorescence light from the analyte atoms in the flame was collected in a perpendicular direction with respect to the DFWM laser beams using a 50 mm focal length lens, focused on the entrance slit of a 20 cm spectrometer (Jobin-Yvon HR20UV) and subsequently detected by a photomultiplier (Hamamatsu R943-02). The fluorescence light was monitored during the alignment procedure in order to simplify the adjustment of laser beam positions and wavelengths.

The signal from the photomultiplier detecting the DFWM light was amplified in a preamplifier (LeCroy VV100B) before being fed into a boxcar amplifier (SR250). The boxcar amplifier integrated the signal over approximately 20 ns, i.e., the duration of the laser pulse, in order to reduce the effect of ambient and scattered light. An average integrated over 30 samples from the boxcar was recorded on a strip-chart recorder. The signal could simultaneously be monitored on a fast digital oscilloscope (Tektronix TDS 640).

Measurements were performed on Au, whose energy level diagram is schematically depicted in Fig 2. In the ordinary one-step DFWM experiments, the DFWM process was initiated between the  $5d^{10} 6s^2 S_{1/2}$  ground state and the  $5d^{10} 6p^2 P_{1/2}$  excited state at  $37359 \text{ cm}^{-1}$ , using 267.595 nm light. In the 2S-DFWM experiments, however, light of this wavelength was used to populate the  $5d^{10} 6p^2 P_{1/2}$  excited state, and the DFWM process

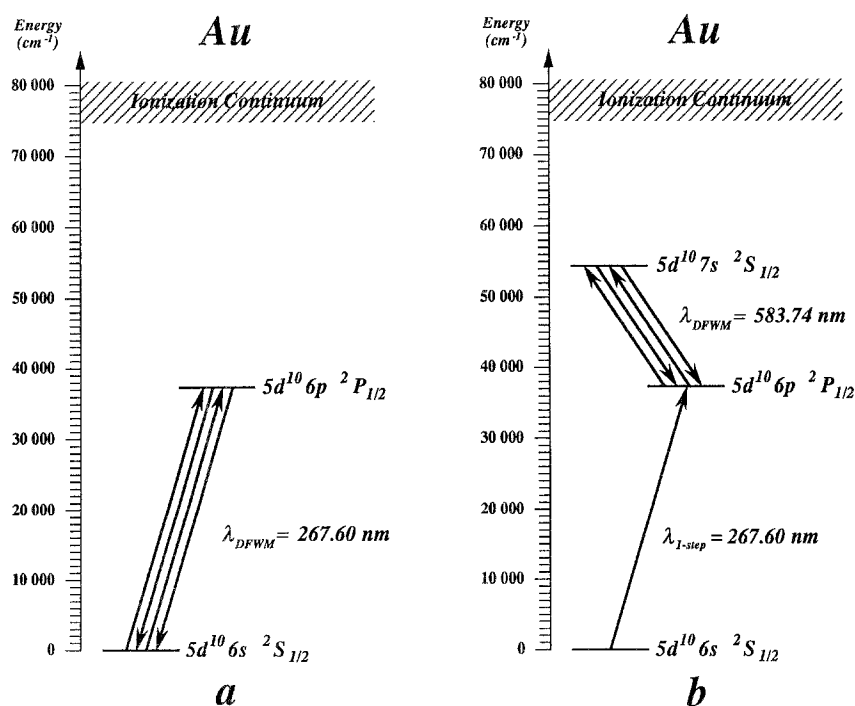


Fig. 2a, b. Schematic energy level diagrams for Au with the transitions used in the ordinary (one-step) DFWM and 2S-DFWM experiments specifically marked

was subsequently initiated between this excited state and the  $5d^{10} 7s^2 S_{1/2}$  excited state at  $54485 \text{ cm}^{-1}$ , using  $583.740 \text{ nm}$  light.

The DFWM pump-beam intensity was around  $9 \text{ kW/cm}^2$  for the ordinary one-step DFWM experiments, which is significantly higher than the DFWM saturation intensity of  $3.7 \text{ kW/cm}^2$  previously measured for this transition [50]. The first-step laser in the 2S-DFWM experiments also had an intensity ( $>4 \text{ kW/cm}^2$ ) significantly exceeding the previously determined population excitation saturation intensity of  $1.1 \text{ kW/cm}^2$  [50]. The intensity of the second step DFWM pump beam in the 2S-DFWM experiments was adjusted for maximum signal quality for each individual experiment, resulting in laser intensities between  $1.6 \text{ kW/cm}^2$  and  $11 \text{ kW/cm}^2$ . This is comparable to the saturation intensity of  $6.0 \text{ kW/cm}^2$  previously measured [50].

## 2 Results and discussion

First, an ordinary (one-step) DFWM signal from Au was studied as a function of Au concentration aspirated into the flame for a parallel experimental arrangement (i.e., with the pump, probe, and signal beams traversing roughly in parallel with each other as well as with respect to the  $10 \text{ cm}$  long flame, creating an elongated interaction region in the middle of the flame). The results are displayed in Fig. 3. In order to more clearly visualize the general trend of the data, a simple phenomenological fit of the form  $S = a (\text{conc})^b / (\text{conc} + c_0)^d$  is included in the plot for modelling the concentration behaviour. In this fit, the concentration dependence for small species densities is mainly given by the parameter  $b$ . The  $c_0$  and the  $d$  parameters are introduced in a phenomenological manner in order to take care of the concentration-saturation behaviour due to pre- and post-filtering effects. As can be clearly seen from the plot as well as the fit, the DFWM signal increases with concentration for lower concentra-

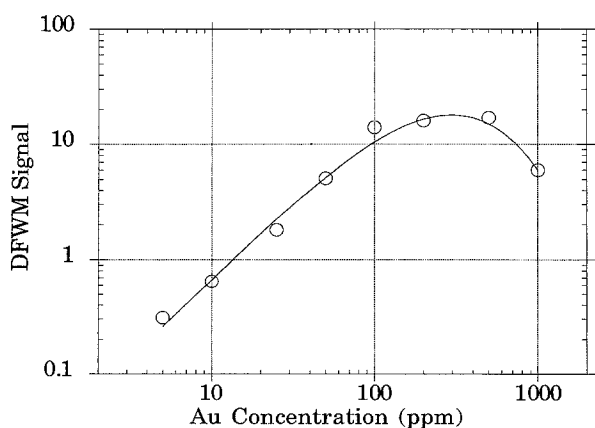


**Fig. 3.** Ordinary (one-step) DFWM signal on resonance as a function of Au concentration for the laser beams and flame in a parallel mode. The laser intensities were  $8.8 \text{ kW/cm}^2$  and  $0.2 \text{ kW/cm}^2$  for the pump and the probe beams, respectively. A phenomenological fit of the type  $S = a (\text{conc})^b / (\text{conc} + c_0)^d$  yields the parameter values  $b = 1.41$ ,  $c_0 = 1450 \text{ ppm}$ , and  $d = 8.33$

tions and “bends over” (i.e., decreases with increasing concentration) for higher concentrations. The reason for this signal decrease for higher concentrations is that pre- and post-filtering absorption effects affect the beams.

For low concentrations the fit gives a power dependence of DFWM signal strength as a function of concentration of 1.4 (i.e.,  $S \propto (\text{conc})^b$  with  $b = 1.41$ ). This is significantly different from the expected quadratic concentration dependence predicted by the simple two-level theory of DFWM [34]. This can be attributed to pre- and post-filtering effects due to absorption of the laser and/or signal beams. Direct evidence of absorption effects could be seen by comparing the DFWM pump beam intensities after passage of the flame with and without aspiration of a  $1000 \text{ ppm}$  Au solution. For this parallel experimental arrangement it was found that the absorption of the pump beam by the aspirated Au atoms for a single passage of the flame was as high as 74%.

In addition, the line-shape of the signal can change drastically with increased concentration due to pre- and post-filtering effects. For DFWM these filtering effects manifest themselves as a dip in the signal exactly at resonance when scanning the laser wavelength across the transition. This behaviour originates from the nonlinear dependence of the DFWM signal upon laser light intensity in combination with an absorption of the incoming laser beams and/or the signal beam that is more and more pronounced the closer to resonance the laser

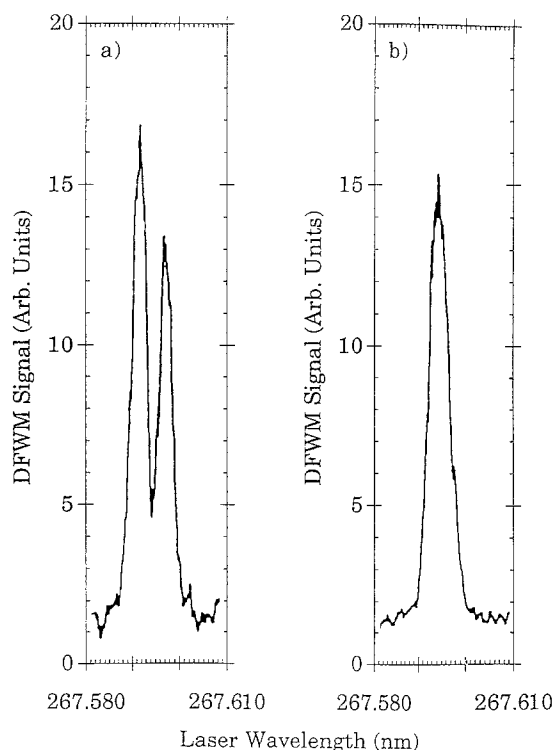


**Fig. 4a, b.** Ordinary (one-step) DFWM signals obtained from a Au solution of  $500 \text{ ppm}$  aspirated into an acetylene/air flame when scanning the laser wavelength across the transition with the laser beams and the flame in a parallel mode (a) and in a perpendicular mode (b), respectively

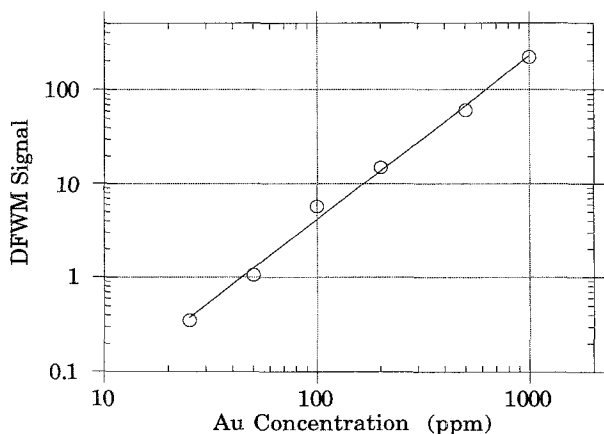


**Fig. 5.** Ordinary (one-step) DFWM signal on resonance as a function of Au concentration for the laser beams and flame in a perpendicular mode. The laser intensities were 8.8 kW/cm<sup>2</sup> and 0.2 kW/cm<sup>2</sup> for the pump and the probe beams, respectively. A simple power-dependence of type  $S = a(\text{conc})^b$  yields a power-dependence of 1.7 ( $b = 1.74$ )

wavelength is tuned. Hence, the line-shape of the DFWM signal can be a double peak structure when not fully optically thin media are probed. Such a double peaked structure is shown in Fig. 4a. This curve represents a scan over the 267.60 nm resonant transition in Au for a 500 ppm solution. As can be clearly seen from the figure, a dip occurs at the resonant wavelength.

One obvious solution to the problem with pre- and post-filtering effects originating from optically thick conditions is to shorten the path-lengths in the medium to be studied. A way of doing this is to turn the elongated flame in a perpendicular direction with respect to the laser beams. A curve-of-growth for one-step DFWM under perpendicular conditions is shown in Fig. 5.

As can be seen from the curve no “bending over” of the curve occurs for higher Au concentrations. Hence, measurements of the species concentration in the actual interaction region can be done with virtually no or negligible pre- or post filtering effects. The absence of pre- and post-filtering effects can also be seen in Fig. 4b which displays a scan across the transition in Au taken under conditions that are virtually identical to those in Fig. 4a, with the only difference being that the flame is positioned perpendicular to the laser beams. The absorption of the DFWM pump beam was in this case found to be 17%.

However, when utilizing optical techniques for studies of other combustion conditions (large scale furnaces, one-cylinder engines, etc) such a solution is not always feasible due to practical limitations. Other ways around the problem are instead to utilize an alternative transition with lower transition probability (smaller absorption cross-section) or to detune the laser wavelength from resonance. Both of these means have disadvantages – suitable alternative transitions do not always exist while wing excitation is potentially more affected by collisional processes than is excitation at the resonance wavelength. Yet another solution, which thus is investigated in more detail in this work, is to utilize 2S-DFWM.

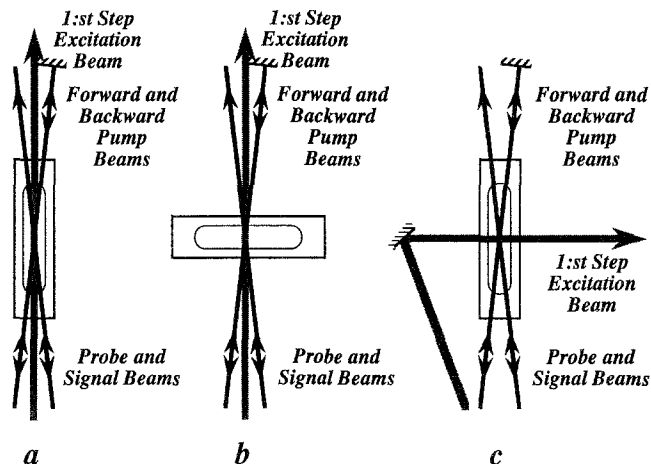


**Fig. 6a–c.** A schematic depiction of the three different geometries used in the 2S-DFWM configurations described below: **a** all laser beams and flame in a parallel geometry; **b** all laser beams parallel with each other, with the flame in a perpendicular mode; **c** the DFWM beams parallel with the flame, with the first-step laser in a perpendicular mode

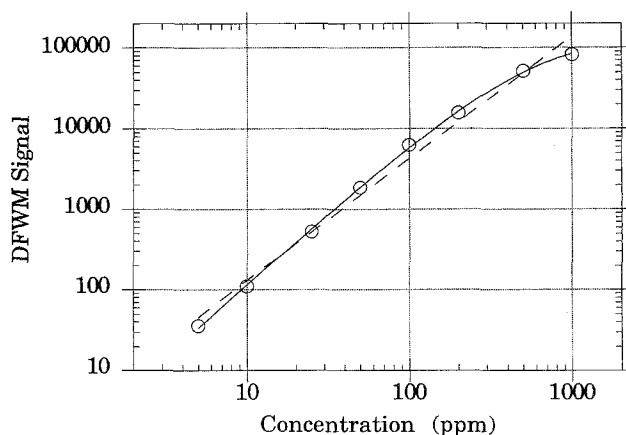


**Fig. 7.** 2S-DFWM signal on resonance as a function of Au concentration for the all-parallel configuration depicted in Fig. 6a. The laser intensities were 1.6 kW/cm<sup>2</sup> and 0.1 kW/cm<sup>2</sup> for the pump and the probe beams, respectively, and 12 kW/cm<sup>2</sup> for the first exciting step. Two fits are inserted with the data. A simple power dependence of type  $S = a(\text{conc})^b$  yields a power-dependence of 1.5 ( $b = 1.51$ ) (dashed line), while a phenomenological fit of the type  $S = a(\text{conc})^b / (\text{conc} + c_0)^d$  yields the parameter values  $b = 1.78$ ,  $c_0 = 1350$  ppm, and  $d = 2.96$  (solid line)

2S-DFWM, i.e., DFWM performed between two excited states of which one (most often the lowest) is populated by excitation of atoms/molecules from lower lying states that have higher thermal populations, has the advantage that pre- and post-filtering effects will be limited to the regions in space where the first (excitation) and the second (DFWM) laser beams overlap.

Hence, a set of 2S-DFWM experiments were performed. Figure 6 summarizes the various geometries that were used in the 2S-DFWM experiments performed, while Figs. 7–9 show some results obtained from experiments performed on Au utilizing the 2S-DFWM technique under similar conditions to the one-step cases above.

Figure 7 presents results obtained from measurements in which the flame was positioned in a parallel mode with respect to all laser beams (i.e., the DFWM pump, probe, and signal beams, as well as the first step exciting laser beam). This corresponds, for the ordinary (one-step) case, to the situation in Fig. 3 above. Since the first-step exciting laser beam is incident at a small angle with respect to the DFWM beams, and thus does not fully overlap the pump and probe beams throughout the flame, a partial reduction of the pre- and post-filtering effects is expected when utilizing this scheme.

As can be seen from Fig. 7, there is no longer any clear evidence for any “bending over” of the signal for higher concentrations. This shows that the major part of the pre- and post-filtering effects indeed has been eliminated. There is still, however, a tendency towards a “levelling-off” of the signal for high concentrations. This indicates that although the pre- and post-filtering effects have been significantly reduced, the fact that the beams still overlap in parts of the flame outside the actual DFWM interaction region prevents a complete elimination of these effects.

The influence of these effects can also be seen by noting that an attempt to fit a power curve of type  $S = a(\text{conc})^b$  to the data, as predicted by a simple two-level system description of DFWM under optically thin conditions, yields a power-dependence of 1.5 ( $b = 1.51$ ). This fit is the straight line shown in Fig. 7. This is again significantly different from the expected quadratic concentration dependence [34].

As can be seen from the figure, there is a discrepancy between the power-fit and the experimental data inasmuch as there is a levelling-off of the experimental data for higher concentrations that is not modelled by the fit. A power-fit throughout the entire concentration range will thus not correctly model the data taken at lower species densities (where pre- and post-filtering effects are expected to play a minor role). A remedy for this is to fit the data to the same type of phenomenological function as used for the one-step DFWM data presented in Fig. 3, i.e.,  $S = a(\text{conc})^b / (\text{conc} + c_0)^d$ . A fit to the data in Figure 7 (i.e., the slightly bent curve in the figure) yields a concentration dependence for low species density situations of 1.8 ( $b = 1.78$ ). This is closer to the expected quadratic concentration behaviour. However, at the same time this fit also gives evidence that some pre- and post filtering effects still remain even at lower species densities.

Signals from a set of measurements from a perpendicular flame configuration utilizing the 2S-DFWM technique is displayed in Fig. 8. Here, we can clearly see that all tendencies of “levelling-off” or “bending over” have disappeared. This is also supported by the fact that the best power-fit yields a nearly pure quadratic dependence ( $b = 2.02$ ). This indicates that the pre- and post-filtering effects have been completely eliminated within this beam and flame geometry.

However, as was argued above, simply turning the flame into a perpendicular mode cannot be seen as a satisfactory solution for many practical applications of

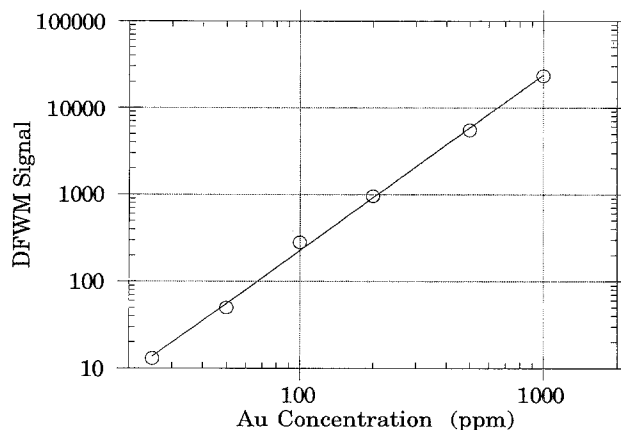


Fig. 8. 2S-DFWM signal on resonance as a function of Au concentration for the geometry with the flame perpendicular to all the laser beams as depicted in Fig. 6b. The laser intensities were 11 kW/cm<sup>2</sup> and 0.6 kW/cm<sup>2</sup> for the pump and the probe beams, respectively, and 5.3 kW/cm<sup>2</sup> for the first exciting step

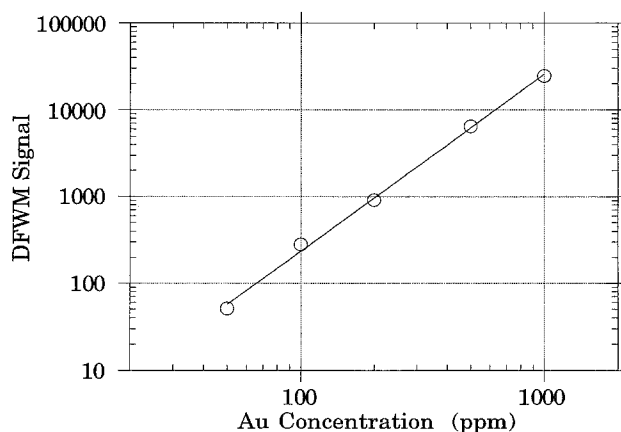


Fig. 9. 2S-DFWM signal on resonance as a function of Au concentration for the case with the DFWM beams parallel with the flame but perpendicular to the first-step excitation beam as depicted in Fig. 6c. The laser intensities were 6.9 kW/cm<sup>2</sup> and 0.4 kW/cm<sup>2</sup> for the pump and the probe beams, respectively, and 4.6 kW/cm<sup>2</sup> for the first exciting step

the DFWM technique. Therefore, further work with the reduction of pre- and post-filtering effects were performed, leading to an investigation of the concept of utilizing crossed laser beams (i.e., using a large angle, e.g., 90°, between the first-step (exciting) laser beam and the second-step (DFWM) beams). Such a configuration is expected to have the property of eliminating virtually all these types of effects since almost no excited atoms, capable of absorbing any significant fraction of any of the four DFWM beams, exist outside of the actual interaction region. Figure 9 therefore finally displays the signals obtained with crossed laser beams (and the flame again parallel with the DFWM beams). What is found is that the signal indeed has a quadratic concentration behaviour ( $b = 2.04$ ), despite the fact that the DFWM beams have traversed a considerable length of the flame.

Consequently, we can conclude that all pre- and post-filtering effects have been eliminated even in the case with parallel flame and DFWM beams by the use of the crossed beam 2S-DFWM technique.

Furthermore, the crossed beam 2S-DFWM technique has the advantage of increasing the spatial resolution of point-measurements performed in the flame by reducing the length of the interaction region to the diameter of the first-step exciting laser. The interaction volume, and hence the spatial resolution, can thus be easily controlled by utilizing suitable lens and aperture configurations.

The drawback of utilizing the crossed beam 2S-DFWM technique is the fact that the reduction in DFWM interaction length, which is responsible for the reduction of pre- and post-filtering effects, also results in a significant decrease in signal strength. By rotating the flame from a parallel to a perpendicular configuration (with parallel first-step (exciting) and DFWM beams, see Figs. 6a, b), the signal strength was reduced by roughly one order of magnitude. When switching to the crossed beam configuration (Fig. 6c) a further reduction of the signal strength by an additional order of magnitude resulted. However, this is not expected to be a major problem for practical measurements in most cases, since the pre- and post-filtering effects that are to be eliminated by utilizing this scheme only appear at such high species concentrations that small signal strengths are generally not a problem. Indeed, in order not to saturate the detection equipment in the present experiments, optical filters had to be introduced in the signal beam path for all our measurements at high concentrations.

### 3 Conclusion

Two-step DFWM (2S-DFWM) is a technique, utilizing two simultaneously pumped dye-lasers, for reduction of pre- and post-filtering effects (originating from partial absorption of the pump, probe or signal beams prior to or after the interaction region) that affect ordinary (one-step) DFWM measurements in media that are not completely optically thin. In the 2S-DFWM technique, the DFWM process is performed between two excited states by utilizing light from one dye laser. Due to the low thermal population of these two states there is negligible absorption of the DFWM laser light in large parts of the media under study. The lower of the two excited states is populated by a laser excitation from a low lying, highly populated state by light from another dye laser. Experiments performed on Au in an acetylene/air flame, comprising a variety of different laser beam and flame configurations, show the usefulness of the 2S-DFWM technique to reduce (or eliminate) severe pre- and post-filtering effects. It is discussed that the crossed beam 2S-DFWM technique also gives the DFWM technique higher spatial resolution. A drawback of the crossed beams 2S-DFWM technique is a decrease in sensitivity.

*Acknowledgements.* This work was supported by the Volvo Research Foundation, project number 92:22, Knut and Alice Wallenberg foundation and Erna and Viktor Hasselblad foundation.

### References

1. R.L. Abrams, J.F. Lam, R.C. Lind, D.G. Steel, P.F. Liao: *Optical Phase Conjugation*, ed. by R.A. Fisher (Academic, New York 1983) pp. 211–284
2. R.L. Farrow, D. Rakestraw: *Science* **257**, 1894 (1992)
3. A.C. Eckbreth, P.A. Bonczyk, J.F. Verdieck: *Prog. Energy Combust. Sci.* **5**, 253 (1979)
4. A.C. Eckbreth: *Laser Diagnostics for Combustion Temperature and Species* (Abacus, Tunbridge Wells, MA 1988)
5. K. Kohse-Höinghaus: *Appl. Phys. B* **50**, 455 (1990)
6. R.K. Hanson, J.M. Seitzman, P.H. Paul: *Appl. Phys. B* **50**, 441 (1990)
7. D.A. Greenhalgh: In *Advances in Nonlinear Spectroscopy*, ed. by R.J.H. Clark, R.E. Hester, Vol. 15 (Wiley, New York 1988)
8. H. Bervas, B. Attal-Trétout, S. Le Boiteux, J.P. Taran: *J. Phys.* **25**, 949 (1992)
9. P. Ewart, S.V. O'Leary: *Opt. Lett.* **11**, 279 (1986)
10. T. Dreier, D.J. Rakestraw: *Opt. Lett.* **15**, 72 (1990)
11. T. Dreier, D.J. Rakestraw: *Appl. Phys. B* **50**, 479 (1990)
12. D.A. Feikema, E. Domingues, M.-J. Cottureau: *Appl. Phys. B* **55**, 424 (1992)
13. M.S. Brown, L.A. Rahn, T. Dreier: *Opt. Lett.* **17**, 76 (1992)
14. R.L. Farrow, D.J. Rakestraw, T. Dreier: *J. Opt. Soc. Am. B* **9**, 1770 (1992)
15. N. Georgiev, U. Westblom, M. Aldén: *Opt. Commun.* **94**, 99 (1992)
16. J. Gumbel, W. Kiefer: *Chem. Phys. Lett.* **189**, 231 (1992)
17. Z. Wu, W.G. Tong: *Anal. Chem.* **65**, 112 (1993)
18. P. Barker, A. Thomas, H. Rubinsztein-Dunlop, O. Axner: *Appl. Phys. B* (submitted)
19. O. Di Lorenzo-Filho, J.R. Rios-Leite: *Chem. Phys. Lett.* **203**, 325 (1993)
20. G. Hall, A.G. Suits, B.J. Whitaker: *Chem. Phys. Lett.* **203**, 277 (1993)
21. R.L. Vander Wal, B.E. Holmes, J.B. Jeffries, P.M. Danehy, R.L. Farrow, D.J. Rakestraw: *Chem. Phys. Lett.* **191**, 251 (1992)
22. J. Pender, L. Hesselink: *Opt. Lett.* **10**, 264 (1985)
23. W.G. Tong, J.M. Andrews, Z. Wu: *Anal. Chem.* **59**, 896 (1987)
24. P. Ewart, P. Snowdon, I. Magnusson: *Opt. Lett.* **14**, 563 (1989)
25. L.J. Rothberg, N. Blombergen: *Phys. Rev. A* **30**, 820 (1984)
26. D.R. Meacher, A. Charlton, P. Ewart, J. Cooper, G. Alber: *Phys. Rev. A* **42**, 3018 (1990)
27. P. Ewart, M. Kaczmarek: *Appl. Opt.* **30**, 3996 (1991)
28. B.A. Mann, S.V. O'Leary, A.G. Astill, D.A. Greenhalgh: *Appl. Phys. B* **54**, 271 (1992)
29. B. Yip, P.M. Danehy, R.K. Hanson: *Opt. Lett.* **15**, 751 (1992)
30. P. Ewart, P. Snowdon: *Opt. Lett.* **15**, 1403 (1990)
31. T.G. Nolan, L.B. Koutny, P.R. Blazewicz, W.B. Whitten, J.M. Ramsey: *Appl. Spectrosc.* **42**, 1045 (1988)
32. J.M. Andrews, W.G. Tong: *Spectrochim. Acta* **44B**, 101 (1989)
33. Z. Wu, W.G. Tong: *Spectrochim. Acta* **47B**, 449 (1992)
34. R.L. Abrams, R.C. Lind: *Opt. Lett.* **2**, 94 (1978)
35. G. Alber, J. Cooper, P. Ewart: *Phys. Rev. A* **31**, 2344 (1985)
36. M.R. Belic: *Phys. Rev. A* **31**, 3169 (1985)
37. P.M. Petersen: *J. Lumin.* **40&41**, 547 (1988)
38. J. Cooper, A. Charlton, D.R. Meacher, P. Ewart, G. Alber: *Phys. Rev. A* **40**, 5705 (1989)
39. H.Y. Ding, B.S. Wu, D.J. Yin, J.Q. Li: *Chin. Phys.* **9**, 369 (1989)
40. D.R. Meacher, P.G.R. Smith, P. Ewart: *Phys. Rev. A* **46**, 2718 (1992)
41. C. Th. J. Alkemade, Tj. Hollander, W. Snellman, P.J. Th. Zeegers: *Metal Vapours in Flames* (Pergamon, Oxford 1982)
42. C. Th. J. Alkemade: *Spectrochim. Acta* **40B**, 1331 (1985)

43. D.J. Butcher, J.P. Dougherty, F.R. Preli, A.P. Walton, G.-T. Wei, R.L. Irwin, R.G. Michel: *J. Anal. At. Spectrom.* **3**, 1059 (1988)
44. J.M. Ramsey, W.B. Whitten: *Anal. Chem.* **59**, 167 (1987)
45. P. Ewart, A.I. Ferguson, S.V. O'Leary: *Opt. Commun.* **40**, 147 (1981)
46. P. Ewart, S.V. O'Leary: *J. Phys. B* **15**, 3669 (1982)
47. P. Ewart, S.V. O'Leary: *J. Phys. B* **17**, 4595 (1984)
48. P. Ewart, S.V. O'Leary: *J. Phys. B* **17**, 4609 (1984)
49. Q. Zhang, S.A. Kandel, T.A.W. Wasserman, P.H. Vaccaro: *J. Chem. Phys.* **96**, 1640 (1992)
50. P. Ljungberg, O. Axner: *Appl. Opt.* (submitted)